

## Dose Evaluation of a Car Occupant in Dual Energy X-Ray Automobile Inspection System

**Mahdi Kahani\* and Samaneh Hashemi**

*Department of Medical Radiation, Shahid Beheshti University, Tehran, Iran*

**\*Corresponding Author:** Mahdi Kahani, Department of Medical Radiation, Shahid Beheshti University, Tehran, Iran.

**Received:** March 11, 2022; **Published:** March 29, 2022

### Abstract

The aim of this study is to assess the risk of car passengers in Dual Energy X-ray inspection devices and to determine the maximum number of passes through the system in a given amount of time. The MCNPX code was used to simulate a newly fabricated dual-energy X-ray car inspection device, which included an X-ray tube, detector arrays, and a rando phantom, to their exact specifications. A Rando phantom was placed in a car and TLD dosimeters were placed within different sections of the phantom for experimental dosimetry. The maximum equivalent dose was absorbed in the gastric, breast, and lungs in experimental results, while simulation results showed that this quantity belongs to bone surfaces and gastric. Based on simulation results and experimental dosimetry, the total equivalent dose of 155 kVp is 0.256 and 0.276 Sv, respectively, with a difference of 7%. The results showed that the MCNPX is suitable for dosimetry in this case. The system falls into the category of devices of limited utility, according to the ANSI standard. Anyone can move through this machine a maximum of 806, 66, and 15 times in a year, month, and week.

**Keywords:** Dual-Energy X-ray; Inspection Devices; Monte Carlo Simulation; TLD Dosimetry

### Introduction

Combating contraband smuggling, especially drug as well as terrorism, by conducting thorough inspections of postal shipments, passenger bags, and vehicles, particularly at borders, is critical to all countries' security and economy. A radiation solution has been suggested and used for a long time to solve this problem and improve protection. In these applications, X-ray scanning systems are commonly used. In the case of drugs with a low atomic number, as well as many explosives such as plastic explosives that can be manufactured and hidden in a variety of types and ways, diagnosis of the substance type, as well as the shapes of objects, is needed [1]; so dual-energy X-ray imaging and a variety of data and image processing algorithms are used in various ways.

Today, as a non-destructive and non-invasive testing method for shape and material identification, this method is very common and reliable. Bone density calculation and contrast agent detection in radiography images are examples of a related approach used in medicine [2-5]. Due to the possibility of several passes from inspection, a person's absorbed dose is extremely important, much as it is in medical applications. Based on the individual's deposited dose per inspection and annual dose restriction, international radiation safety organizations have determined the maximum number of times a person can pass through the system. In this regard, the US national standard has given some tables that can be useful if the scan is fully justified [6]. As a result, every new inspection system would need to assess and calculate the average whole-body dose and the dose of the organ at risk.

Although a large portion of the personal dose is due to inevitable accidental exposure, the dose from human activities such as medical, industrial, and inspection is substantial and should be taken into account, according to ICRP standards [7]. Different inspection device parameters, such as the X-ray tube's radiation spectrum, imaging geometry, materials, and other effective parameters, show that dosimetry is needed for each X-ray inspection device. The beam energy of these devices can be adjusted for cars, containers,

and even trains, and they can be fixed or portable [8]. Khan et al. published a detailed report in 2003 on the dose received by humans during container inspection at US borders and with various forms of inspection cargo equipment. A Rando man equivalent phantom and TLD dosimeters were used to measure dose in this study [8]. One of the study's most intriguing findings was that the absorbed dose is unaffected by the person's location (sitting or standing). Hope et al. stated in 2005 that the dose received by people during individual X-ray inspections ranged from 0.07 to 6 Sv [9]. While several studies have looked at the personal absorbed dose in a container or during an individual inspection, this study will look at the personal dose of a person sitting in a car as it passes through a dual-energy X-ray inspection system.

X-ray inspection systems for cars and containers range in energy from 100 kVp X-ray tube output (similar to the fabricated system for this study) to 10 MeV linear accelerator output [10-12], with different results in terms of personal absorbed dose, detection precision, and application range. Based on the average dose per scan of a car passenger, the aim of this study was to calculate the maximum number of passing through the car inspection system in the allotted time.

## Materials and Methods

### Fabricated Imaging System

In this study, an XRB401 model of X-ray tube from Spellman Company was used, as well as an array detector from Detection Technology Company's X-card 2.5-64DE model. Their specifications are mentioned in Table 1. Figure 1 shows a diagram of the imaging device configuration.

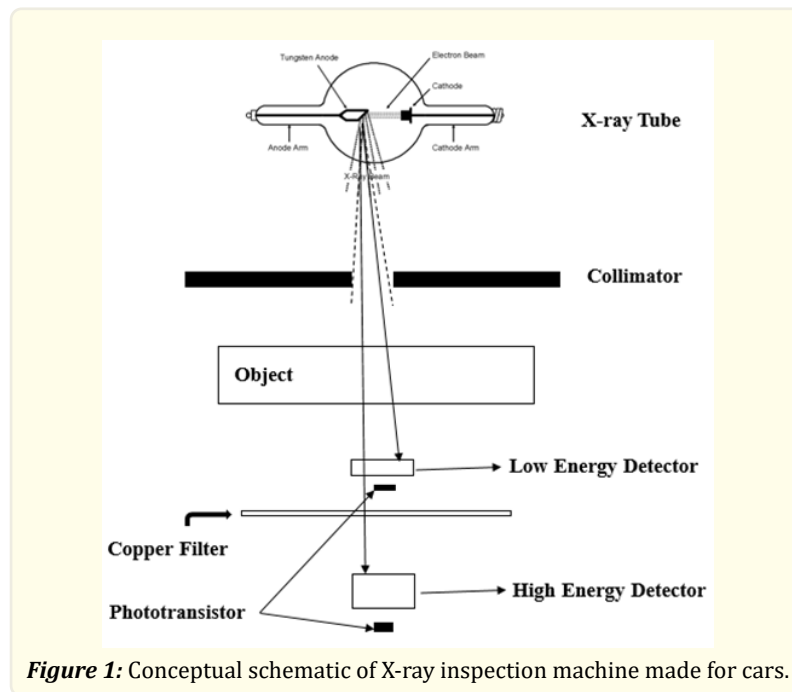


Figure 1: Conceptual schematic of X-ray inspection machine made for cars.

<i>X-ray tube &amp; Detector array</i>	
2.49 mm	Pixel pitch
GOS sheet, 145 mg/cm <sup>2</sup> DRZ screen thickness:0.3 mm	Scintillator of low energy detector
Copper: 0.6 mm	Filter among the low & high energy detector
CsI(Tl) Crystal thickness: 3 mm/4 mm	Scintillator of high energy detector
1536 Pixel	Total range of detector
50-200 kVp	Tube's energy range
0.2-2 mA	mA range
Fan Beam	X-ray's beam output shape

**Table1:** Detector and X-ray tube specifications in fabricated X-ray car inspection machine.

The main objective of this device's construction was to provide imaging capability while maintaining adequate inspection object quality, as well as material classification into organic and inorganic categories. Figure 2 shows a view of the inspection machine. Also visible in the results image and in figure 5 as the final response to the material classification algorithm is an example of a scanned car image containing a small drug in its trunk, underneath a chair, and into another chair, as well as a gun. The orange color spectrum in this picture represents organic matter, while the gray spectrum represents non-organic matter. The atomic number map's logarithmic approach was used to perform the material classification algorithm.



**Figure 2:** A picture of dual energy X-ray car inspection machine made in Iran.

### **MCNPX Monte Carlo Simulation**

Initially, dose evaluations of the car passenger were performed using the MCNPX 2.6 Monte Carlo (MC) code to simulate all of the system geometry and materials. The Monte Carlo N-Particle extended (MCNPX) code, created by Los Alamos National Laboratory in the United States, is a general-purpose MC code for radiation transport simulation that has applications in nuclear, manufacturing, and medical simulations. The MC code solves particle transport problems statistically, and the results are per particle. As a result, dosimetries in various parts of the human body do not have many experimental restrictions, such as placing dosimeters in different body organs and repeating the procedure under different conditions; thus, the MCNPX code may be a useful tool in this regard. This code has been used to simulate dual-energy X-ray imaging and dosimetry in several studies [13-16].

To calculate the effective dose of body's different organs in this study, an anthropomorphic phantom was used to mimic the human body in the MCNP MC code. The mathematical phantom of ORNL, which was originally specified to calculate the medical internal radiation dose (MIRD), was employed for dosimetry. The phantom can be seen in figure 3 in three different views. This phantom uses

mathematical definitions and shapes to describe the different organs of the body as normal ones. Despite the fact that this phantom are easily discernible from humans, their intent is to be hermaphroditic and modeled on reference and human masses [17]. The X-ray tube was modeled as a point source, with the energy spectrum derived using the validated report IPEM 78 [2, 18] based on the X-ray tube specifications of inspection system. \*F8 tally of MCNPX was used to calculate doses in different organs such as brain, thyroid, Salivary glands, breast, and et cetera. The output of this tally is the abundance of energy recorded in each cell which is expressed in MeV and must be divided by the cell's unit mass to achieve the dose. The results were reported with less than 5% error using a personal computer with four processor cores. Some corrections were made to all of the simulated parameters in order to optimize the accuracy between the experimental dosimetry geometry and the simulation, as well as to compare simulation and experimental results and unify their scales.

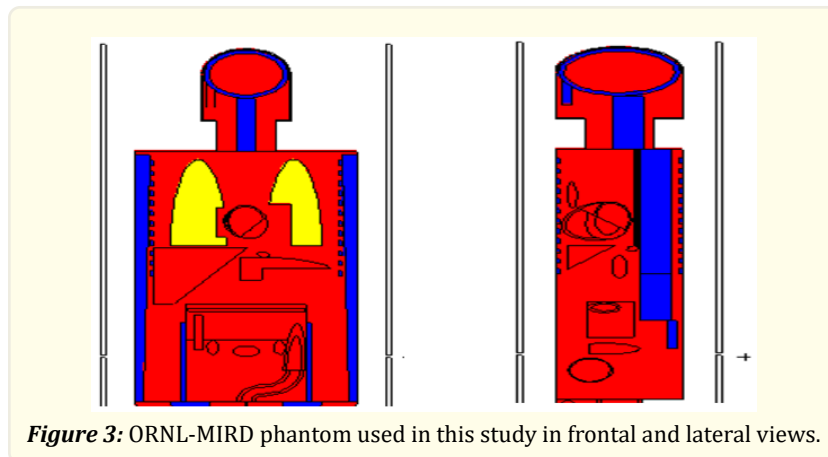


Figure 3: ORNL-MIRD phantom used in this study in frontal and lateral views.

### Experimental Dosimetry

In the experimental dosimetry, a Rando phantom was used to test the experimental dose of the vehicle's occupant. The equivalent dose for each organ was determined by placing dosimeters at a depth of 10 mm, and the effective dose was determined by applying each tissue's weighting factors [19]. All dosimetries were performed with the same X-ray tube current of 1 mA and a 155 kVp energy. TLD type and LiF(Mg, Cu, P) model dosimeters were manufactured in China under the GR-200 brand name. Based on a detailed analysis by Del Sol Fernandez et al., this TLD has a higher sensitivity (approximately 66%) and better dosimetric properties than the TLD-100, which found that the TLD-100 is inaccurate for measurements below 4mGy [20]. Each dosimeter had a diameter of 4.9 mm and a thickness of 9 mm, with a total of 82 dosimeters used in the phantom. Table 2 shows the radiation weighting factors [21] in various body tissues as well as the distribution of dosimeter numbers in the Rando phantom. The calibration process was done by Elekta Precise Linear Accelerator (Elekta Precise model, Germany) and 6 MeVphoton beam with 50 cGy dose. A 3500 TLD reader (Harshaw-Bicron, USA) was used to read the TLD pieces.

To minimize the error between the simulation and experimental results, the experimental coefficients were determined by putting the phantom alone under the X-ray tube exposure and comparing the findings to those of the simulation. The phantom was then placed in the car and passed through the inspection system, and dosimetry was performed as a car occupant by using the experimental coefficients. The experimental coefficients of 1.14 and 1.22 were obtained at energies of 175 and 195 kVp, respectively. The phantom was then placed in the car, and dosimetry was performed using the experimental coefficients as a car occupant.

The vehicle's speed is about 10-15 km/h. The system gate's RF receivers detect the car approaching location and activate the device. The radiation lasts 2 seconds, and it will finish in 2 seconds even if the car comes to a halt at the gate for some reason. The device's alarm lights illuminate when it is turned on. The user has control over the X-ray source parameters (voltage and current) and can adjust them to suit the situation. The phantom was stowed behind the driver's seat. The condition of an average mid-sized person in the

sitting position is simulated on the car seat with this configuration, and since all areas inside the car's cabin receive approximately the same dose rate, this calculation may be called an occupant's dose index for all cabin areas. This is because of the X-ray tube and detector are located at the top and bottom of the car inspection device, respectively, and the only buffer between the occupant and the X-ray tube is the car's roof. Since the roof thickness is consistent throughout, it is expected that all occupants will receive the same dose.

Moreover, different automobiles were used for dosimetries because changing the dose of a car passenger is possible by changing the type and model of the car. To minimize statistical error and improve the accuracy of the results, 103 scans/dosimetry were performed, with the average of the results recorded. Figure 4 depicts a used Rando phantom and its location inside the vehicle.

<i>Tissue Type</i>	<i>Tissue Weighting Factors</i>	<i>Dosimeters Number</i>	<i>Tissue Type</i>	<i>Tissue Weighting Factors</i>	<i>Dosimeters Number</i>
<i>Brain</i>	0.01	3	<i>Gonads</i>	0.08	2
<i>Esophagus</i>	0.04	3	<i>Skin</i>	0.01	6
<i>Thyroid</i>	0.04	6	<i>Eye lens</i>		2
<i>Salivary glands</i>	0.01	2	<i>Bone marrow</i>	0.12	4
<i>Bone surface</i>	0.01	4	<i>Colon</i>	0.12	4
<i>Lung</i>	0.14	14	<i>Liver</i>	0.04	9
<i>Breast</i>	0.12	8	<i>Other organs</i>	0.12	10
<i>Gastric</i>	0.12	3	<i>Total</i>	1	8
<i>Bladder</i>	0.04	2			

**Table 2:** Body tissue weighting factors, as well as the number distribution of dosimeters inserted in the Rando phantom.



**Figure 4:** Rando phantom placement along with dosimeters planted inside it and on its surface, in the same position as ordinary people at the time of scanning.

## Results and discussion

Table 3 shows the results of the simulation using the MC code for 155 kVp energy. Based on these findings, the lungs, bone surface, and gastric received the largest absorbed doses of 0.0486, 0.0416, and 0.0406  $\mu\text{Sv}$ , respectively. Furthermore, the average cumulative received dose for this energy by car passengers was 0.2564  $\mu\text{Sv}$ , which is very low as compared to the annual allowable dose for individuals. As a result, it can effectively reduce concerns about an occupant's absorbed dose, but the exact amount of passes through the system should be regarded. Glands, especially gonads, have been identified as one of the most ionizing radiation-sensitive tissues. Both

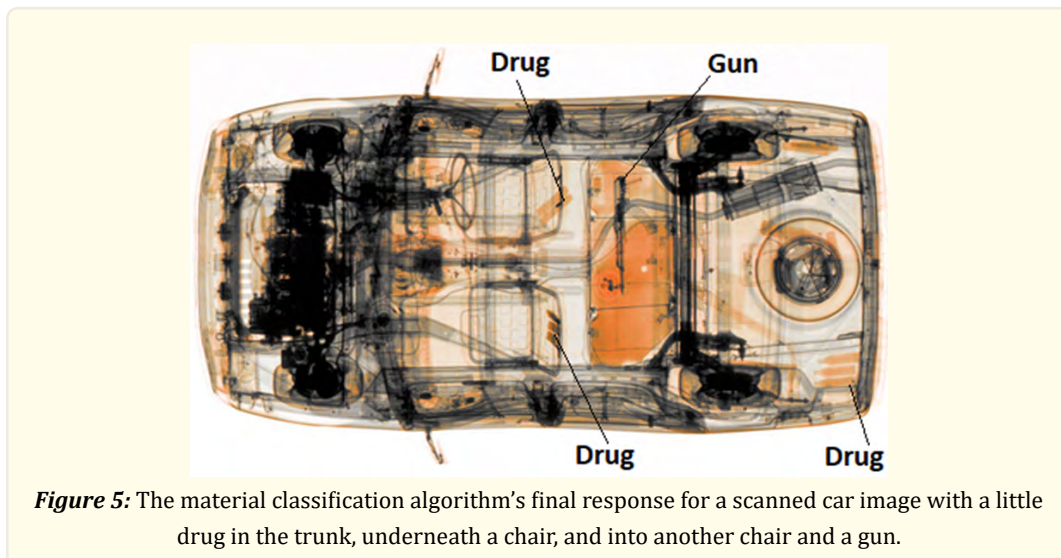
of these issues are essentially addressed by dose measurements of 0.0001 and 0.0160  $\mu\text{Sv}$  in simulation and experimental dosimetry, respectively. The simulation results show that the minimum dose is linked to salivary glands, gonads, and bone marrow, respectively.

The effects of experimental dosimeters using the TLD and the equivalent human phantom for each organ, individually and for the entire body, have been measured and are referred to as "Effective doses." According to these findings, the minimum dose of 155 kVp energy belongs to the skin surface and bone surface, and it is equivalent to 0.0024  $\mu\text{Sv}$ . With a dose of 0.044  $\mu\text{Sv}$  in the gastric and other organs, the highest effective dose was achieved. The average effective dose obtained in this energy is 0.276  $\mu\text{Sv}$ , based on these findings. In addition, as X-ray energy increases, the average effective dose rises. As a result, the effective dose for a car's occupant was 0.315 and 0.338  $\mu\text{Sv}$  for 175 and 195 kVp energy, respectively.

Figure 6 depicts a comparison of simulation results and practical dosimetries. As can be seen, the results from both methods are highly correlated in many organs and the total absorbed dose. The difference in average passenger dose between the two methods for 155 kVp energy is 7%, demonstrating that the MCNPX code is justified and accurate in this application. Despite the small differences between simulation and experimental results for the overall effective dose, it should be noted that the dose in individual organs differed greatly, particularly in smaller organs. If it's because there aren't enough simulated events.

Khan et. al. conducted a thorough investigation in 2004 into seven cargo, railroad, or truck inspection systems that used X-ray, Gamma, and neutron to identify materials [7]. Low-energy X-ray devices had energies of 420-450 kVp and currents of 6.6-10 mA, with relative doses of 0.4-2.3  $\mu\text{Sv}$ . Hupe et. al. (2006) recorded 0.2 and 0.4  $\mu\text{Sv}$  received dose using 450 kVp and 6.6 mA in two fast and slow modes [14]. The obtained doses are found to be minor but not zero, and are dependent on energy, current, scan time, and geometry.

In the case of trucks, one method of lowering the driver's dose is to avoid direct exposure. The driver's exposure is only due to scattered radiation from the truck's load inspection in this case [22]. Although this operation cannot be carried out during a car inspection, a robust and automated conveyor for the car going through the device's gate is recommended to protect passengers. Furthermore, since the passenger's irradiation period on these devices is very short and the obtained dose is dependent on time, the passenger dose decreases as a result. Moreover, by adjusting the form of vehicles, a difference of 0.2 to 0.55  $\mu\text{Sv}$  was measured in the average dose.



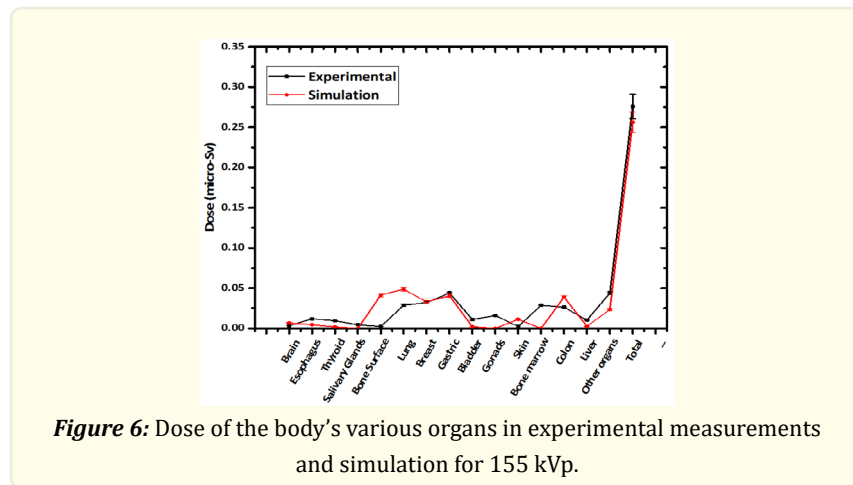


Figure 6: Dose of the body's various organs in experimental measurements and simulation for 155 kVp.

The American National Standards Institute (ANSI) divides X-ray inspection systems into two categories: general application and limited use. Generic devices are those in which each person's effective dose per scan is less than 0.25  $\mu\text{Sv}$ , and the cumulative personal dose received over a year is less than 250  $\mu\text{Sv}$ . Limited devices are those in which each person's effective dose per scan is more than 0.25  $\mu\text{Sv}$  and less than 10  $\mu\text{Sv}$ , and the total received dose is less than 250  $\mu\text{Sv}$  per year.

Table 3 shows that the examined device falls into the restricted application group when considering the average effective dose of a person going through the machine based on experimental dosimetry results per scan time (0.31  $\mu\text{Sv}$ ). The United States National Standard [6] provided this table with complete justification for performing the scan. The allowable number of passes for each person from this system for one year, one month, and one week is equal to 806, 66, and 15, respectively, using the LabFit program and ensuring that the data is correctly fitted with the "ChiSq" test. An individual who adheres to this standard will not be permitted to exceed these figures.

<i>Effective individual dose per scan (<math>\mu\text{Sv}</math>)</i>	<i>Maximum number of annual scan</i>	<i>Average number of scans per month for not exceeding the maximum allowed for a year</i>	<i>Average number of scans per week for not exceeding the maximum allowed for a year</i>
0.05	5000	416	96
0.10	2500	208	48
0.15	1667	138	32
0.20	1250	104	24
0.25	1000	83	19
0.31*	806	66	15
0.5	500	41	9
1.0	250	20	4
2.0	125	10	2
3.0	80	6	1
4.0	62	5	1
5.0	50	4	
10.0	25	2	

\*The average equivalent dose of the system studied in this research was calculated using interpolation in the ANSI table. It's also worth noting that all measurements are done at a speed of 10 km/h, and the dose obtained by the person varies linearly with the vehicle's speed.

Table 3: The maximum number of scans allowed for different values of the individual dose in each inspection scan [6].

## Conclusion

The findings of this study show that the MCNPX MC code is a useful and trustworthy method for X-ray car inspection. It was also discovered that using TLD dosimeters in conjunction with a Rando-MIRD phantom in a dual-energy X-ray car inspection machine allows for material classification. Furthermore, according to ANSI standards, the fabricated machine is a restricted application unit, and a person can be scanned a maximum of 806, 66, and 15 times per year, week, and month, respectively, if the scan is completely justified.

## References

1. Eilbert RF and Krug KD. "Aspects of image recognition in Vivid Technologies' dual-energy x-ray system for explosives detection". *Applications of Signal and Image Processing in Explosives Detection Systems*. International Society for Optics and Photonics 1824 (1993): 127-144.
2. Kahani M, Kamali-asl A, Ghadiri H and Hashemi S. "A method for material decomposition in dual-energy contrast enhancement digital mammography". *Measurement* 88 (2016): 87-95.
3. Mazess RB, Barden HS, Bisek JP and Hanson J. "Dual-energy x-ray absorptiometry for total-body and regional bone-mineral and soft-tissue composition". *The American journal of clinical nutrition* 51.6 (1990): 1106-1112.
4. Kahani M, Mahdi M, KamaliAsl A, Hashemi S and Ghadiri H. "Simultaneous Use of Two Different Contrast Agents and Assessing their Accuracy in Breast Tissue Using Dual-Energy Digital Mammography". *Journal of Mazandaran University of Medical Sciences* 24.122 (2015): 239-251.
5. Mojorad Kahani M, Kamali A, Hashemi S and Ghadiri H. "Automatic Detection of Micro-Calcification in Breast Tissue by X-Ray Dual-energy Technique for Early Detection of Breast Cancer". *Journal of Mazandaran University of Medical Sciences* 24.116 (2014): 11-22.
6. American National Standard for Determination of the Imaging Performance of X-Ray and Gamma-Ray Systems for Cargo and Vehicle Screening ANSI N42 46-2008, American National Standards Institute, Institute of Electrical and Electronics Engineers (IEEE) (2008).
7. Khan SM, Nicholas PE and Terpilak MS. "Radiation dose equivalent to stowaways in vehicles". *Health physics* 86.5 (2004): 483-492.
8. Blish RC, Li SX and Lehtonen D. "Filter optimization for X-ray inspection of surface-mounted ICs". *IEEE Transactions on device and materials reliability* 2.4 (2002): 102-106.
9. Zavadtsev AA., et al. "A dual-energylinac cargo inspection system". *Instruments and Experimental Techniques* 54.2 (2011): 241-248.
10. Macdonald RD. "Design and implementation of a dual-energy X-ray imaging system for organic material detection in an airport security application". *Machine Vision Applications in Industrial Inspection IX*. International Society for Optics and Photonics 4301 (2001): 31-42.
11. Cember H. *Introduction to health physics*. Introduction to health physics (1969).
12. Maharaj HP. "Predicting absorbed doses and risks from some inspection X-ray machines". *Journal of Radiological Protection* 15.4 (1995): 303.
13. Kahani M, Kamali-Asl A and Tabrizi SH. "Proposition of a practical protocol for obtaining a valid radiology image using radiography tally of MCNPX Monte Carlo Code". *Applied Radiation and Isotopes* 149 (2019): 114-22.
14. Hashemi S, Aghamiri MR, Kahani M and Jaberri R. "Investigation of gold nanoparticle effects in brachytherapy by an electron emitter ophthalmic plaque". *International Journal of Nanomedicine* 14 (2019): 4157.
15. Kahani M, Tabrizi SH, Kamali-Asl A and Hashemi S. "A novel approach to classify urinary stones using dual-energy kidney, ureter and bladder (DEKUB) X-ray imaging". *Applied Radiation and Isotopes* (2020): 109267.
16. Hashemi S, Aghamiri SM, Jaberri R, Siavashpour Z. "An in silico study on the effect of host tissue at brachytherapy dose enhancement by gold nanoparticles". *Brachytherapy* 20.2 (2021): 420-5.

17. Harrison John D. "Phantom Evolution". (2020): 7-11.
18. Khabaz R. "Phantom dosimetry and cancer risks estimation undergoing 6 MV photon beam by an Elekta SL-25 linac". Applied Radiation and Isotopes 163 (2020): 109232.
19. Reilly AJ, Sutton D. IPEM Report 78-Spectrum processor. York: The Institute of Physics and Engineering in Medicine (1997).
20. Hupe O and Ankerhold U. "Determination of ambient and personal dose equivalent for personnel and cargo security screening". Radiation protection dosimetry 121.4 (2006): 429-437.
21. Fernandez SD, García-Salcedo R, Mendoza JG, Sánchez-Guzmán D, Rodríguez GR, Gaona E and Montalvo TR. "Thermoluminescent characteristics of LiF: Mg, Cu, P and CaSO<sub>4</sub>: Dy for low dose measurement". Applied Radiation and Isotopes 111 (2016): 50-5.
22. Protection R. ICRP publication 103. Ann ICRP 37.2.4 (2007): 2.
23. Gomes RS, Gomes JD, Costa MLL and Miranda MVF. "Dose to drivers during drive-through cargo scanning using GEANT4 Monte Carlo simulation". International Nuclear Atlantic Conference - INAC 2013 Recife, PE, Brazil (2013).

**Volume 2 Issue 4 April 2022**

**© All rights are reserved by Mahdi Kahani., et al.**